J. Phys.: Condens. Matter **11** (1999) 383–404. Printed in the UK PII: S0953-8984(99)97239-9

Tunnelling and point contact spectroscopy of the density of states in quasicrystalline alloys

R Escudero†, J C Lasjaunias‡, Y Calvayrac§ and M Boudard‖

† Instituto de Investigaciones en Materiales, Universidad Nacional Autónoma de México, Apartado Postal 70-360, México, DF, 04510, Mexico
‡ Centre de Recherches sur les Très Basses Températures, CNRS, BP 166, 38042 Grenoble Cédex 9, France
§ Centre d'Etudes de Chimie Métallurgique, CNRS, 15 rue Georges Urbain, 94407 Vitry-sur-Seine Cédex, France
‖ Laboratoire de Thermodynamique et de Physico-Chimie Métallurgiques, BP75-38042, Saint Martin-D'Heres Cédex, France

Received 7 September 1998

Abstract. Point contact and tunnelling experiments performed at low temperatures were used to study the electronic behaviour of the icosahedral quasicrystalline alloys AlPdRe, AlCuFe, and AlPdMn. With samples of high quality we observed at low temperatures a zero-bias anomaly that we related to the decrease of the electronic density of states (DOS) due to the electron–electron interaction. This interaction tends to diminish the DOS at the Fermi level and can be seen as the energy pseudogap of the alloy. Our experiments indicate that the DOS is strongly modified near E_F and consists of a spiky feature in a broad pseudogap, with the width of the feature of the order of 100 meV or even larger for the AlPdRe, whereas it is as small as 20–22 meV for Al–Cu–Fe and 17–20 meV for Al–Pd–Mn. The broad pseudogap has widths larger than 400 meV for AlPdRe, whereas for AlCuFe it is about 80–90 meV and for AlPdMn it is of the order of 110–122 meV. The studies were performed on three samples of the compositions $Al_{70.5}Pd_{21}Re_{8.5}$, $Al_{68.2}Pd_{22.8}Mn_{9.0}$, and $Al_{63}Cu_{25}Fe_{12}$. The junctions were of the types alloy–Au(In, Al) and alloy–insulator–Au(In, Al), and were studied at different temperatures between that of liquid nitrogen and 2 K, and even to 400 mK for the AlCuFe alloy.

1. Introduction

From the experimentalist's point of view it is established that for a quasiperiodic structure the physical properties mainly related to the electronic behaviour, e.g. transport properties, clearly indicate that the electronic behaviour is radically different to that occurring in crystalline structures—i.e. resistivity increases when the structural perfection increases; thus, in a very crude approach, by comparison to the situation induced by disorder in metallic alloys, one can speculate that the Anderson localization increases as the quasicrystal (QC) purity and structural perfection increases. The problem of whether the electronic wavefunctions are extended or localized is currently a matter of debate. In any case, it is now clear that the conventional picture of Anderson localization in disordered systems is not relevant to QCs [1–3].

Another interesting experimental result observed for QCs is that found for AlCuFe and AlPdRe, i.e. the high values of the resistivity at low temperatures [1]; this is considered consistent with the presence of a significant reduction of the density of states at the Fermi level. This reduction of the density of states can be assumed to be due to a strong electron–electron interaction [4, 5] which supports the stabilization of the quasicrystalline structure.

0953-8984/99/020383+22$19.50

This feature or pseudogap at the Fermi level has been predicted theoretically by Fujiwara [6] and Fujiwara and Yokokawa [7], in efforts to explain the stability of QC alloys. It is important to mention that the presence of a Hume-Rothery-like pseudogap was predicted a long time ago by Friedel and Dénoyer [8]; this has also been suggested as the origin of the stabilization of QC structures.

Some experimental evidence that reinforces these theoretical assumptions of the existence of a pseudogap can be found in measurements of the specific heat capacity at low temperatures, which indicate a very small electronic density of states (DOS) at the Fermi level, corresponding to a very small electronic term γ, between just 1/4 (for AlCuFe [9, 10]) and ∼1/10 (for AlPdRe [11–14]) of the value for pure aluminium metal. In addition, photoemission [15, 16] and soft x-ray emission spectroscopy [17,18] have revealed the presence of a wide pseudogap of about 1 eV at E_F, in AlPdMn, AlCuFe, and AlPdRe. We note at this stage that one of the most unusual electrical properties of QCs—the very large low-T resistivity of AlPdRe compared to that of AlCuFe—cannot be explained by a corresponding reduction of the electronic DOS at E_F: whereas the resistivity ratio of the two systems can reach a possible value of 100, the reduction in the γ-term is only by about a factor of 2. Other experimental features, such as the relative insensitivity of γ to thermal annealing in contrast to the case for the electrical resistivity [14], confirm that the high resistivity value of high-quality QCs is not of band-structure origin.

In order to test the very important prediction of Fujiwara *et al* [2, 7] that the quasi-periodicity could yield a very spiky fine structure of the electronic DOS over an energy scale of about 10 meV, which could also explain the unusual behaviour of the thermopower and Hall conductivity [2], spectroscopic techniques having better resolution than photoemission or x-ray spectroscopy, usually limited to 0.4–0.5 eV, have to be used. This is the case for high-resolution tunnelling or point contact tunnelling spectroscopy techniques, which are frequently used in solid-state physics to probe features of the electronic DOS close to the Fermi surface, but until now rarely in the case of QCs. It is important to point out that these two techniques have a high resolution which is of the order of k_BT; so at 4 K the resolution may be as good as 0.35 meV.

A first investigation of AlCuFe QC films by scanning tunnelling spectroscopy by Klein *et al* [19] has produced evidence of a narrow gap, 60 meV wide at about 4.2 K. A second STM investigation by Davydov *et al* [20], on AlCuFe and AlPdRe QC ribbons, of better resolution, has confirmed the presence of a pseudogap for $|E| < 50$ meV, but did not show other pseudogaps in the energy region near ∼0.5 eV, or even at energies lower than 50 meV, contrary to the theoretical predictions.

In this paper we will present a comparative study of the electronic structure around the Fermi level, by tunnelling and point contact spectroscopy, of three different QC species of high structural quality, which are characterized by very different electrical transport properties: AlCuFe, AlPdMn, and AlPdRe. With tunnelling spectroscopy we are able to probe in a direct manner the evidence of pseudogap features, and also the variations of the density of states, whereas with point contact spectroscopy we can, at least, observe—but in different form—the features of the pseudogap.

The high-resolution junction devices used here have allowed the study of the temperature dependence of the differential conductance from liquid nitrogen temperature down to about 2 K, and even down to 0.4 K in the case of AlCuFe alloy—information not available from the early STM technique.

With these techniques we are able to observe many of the physical phenomena that occur in the density of states close to the Fermi surface, and, accordingly, to study some of the scattering processes and characteristic features around the Fermi level. The main results of

this work are the following:

(a) The observation of different values of the pseudogap feature for the three different QC alloys studied.
(b) The determination of a spiky feature of small width, superimposed on a broad pseudogap; this broad pseudogap reaches values of several hundreds of mV in some QCs.
(c) The dependence on temperature of the electron–electron Coulomb interaction, at the origin of the pseudogap, which is strong at lower temperatures, and becomes negligible at about 50 K for QCs of AlPdMn and AlCuFe, whereas it remains very strong at 70 K for the QC alloy AlPdRe.
(d) The absence of any fine structure other than that centred at the Fermi energy.

2. Experimental procedure

2.1. Sample preparation and characterization

Firstly, let us summarize the electronic properties of the alloys investigated. The high-quality species of QCs under study show very different electronic characteristics:

(a) AlPdMn (with 9 at.% Mn) has a resistivity close to 10^{-3} Ω cm, not very far from the values for amorphous metallic alloys, with a small overall variation—less than 10% over the temperature range from 4 to 300 K—and with a very-low-T regime governed by magnetic interactions.
(b) AlCuFe shows a low-T resistivity four times that of AlPdMn, with a characteristic negative thermal coefficient corresponding to a resistivity ratio $R = \rho_{4\,\mathrm{K}}/\rho_{300\,\mathrm{K}} = 1.8$.
(c) AlPdRe shows the highest resistivity among these QC species, and a large resistivity ratio, $\rho_{4\,\mathrm{K}}/\rho_{300\,\mathrm{K}}$, which can reach values of 100 to 200, depending on the sample [14, 21].

In this work we used QCs that show ratios between 30 and 100.

In contrast to these marked differences, as outlined above, photoemission or x-ray emission spectroscopy (in general of about 0.3–0.5 eV resolution) did not reveal significant differences among the three species in their electronic DOS near E_F, which were characterized by wide pseudogaps of about 1 eV [16–18, 22].

The results of photoemission studies of better experimental resolution (50 meV in the case of AlPdMn [23] and 0.14 eV for AlCuFe [15]) are also consistent with a broad and smooth pseudogap feature, without any fine spiky structure. Very recent photoemission experiments of very high energy resolution ($\lesssim$10 meV) [24] have confirmed the presence of the pseudogap in the three QC species with a half-width of the dip in the DOS of 0.22, 0.35, and 0.21 eV for AlPdMn, AlCuFe, and AlPdRe icosahedral alloy, respectively. In addition, a Fermi edge is clearly detected at low temperatures, which confirms that the alloys remain metallic. Again, in these studies, the theoretically predicted spikiness of the DOS could not be observed within the 5 meV experimental resolution.

2.1.1. Al–Pd–Mn alloys. The samples used in this study came from a large-size parent rod grown by the Czochralski technique at the Louis Néel Laboratory in Grenoble, France, which has been characterized as single phased, of perfect icosahedral symmetry, with negligible phason disorder. The composition is $Al_{68.2}Pd_{22.8}Mn_{9.0}$ with an uncertainty of ± 0.2 at.% for each element [25]. The resistivity data reported in figure 1 are in general agreement with previous data obtained for melt-spun samples, for similar compositions [26]. The $\rho(T)$ curve is characterized by a weak T-dependence (an overall variation of 8% between 2 and 300 K)

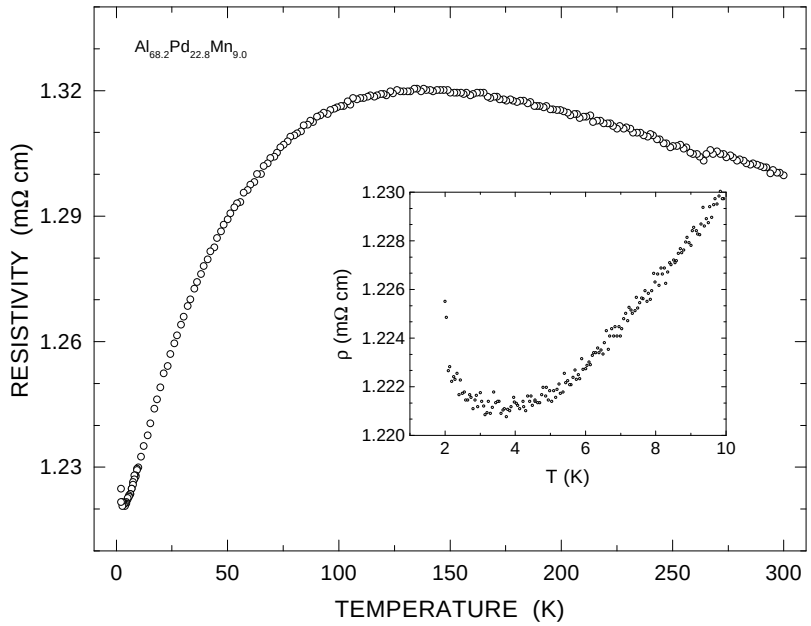

Figure 1. The temperature dependence of the resistivity for i-$Al_{68.2}Pd_{22.8}Mn_{9.0}$. The inset shows the behaviour at low temperature.

and by a broad maximum around 150 K. As reported by Lanco *et al* [26], there is an upturn in the helium T-range, which is ascribed to magnetic scattering by the localized Mn moments; see figure 1, inset. Indeed the DC susceptibility data measured with a field of 10^3 G for this sample reported on in figure 2(a) are in good correspondence with those obtained for an AlPdMn (9.6 at.%) single-grain sample, widely investigated by magnetic and specific heat techniques [27]. There is a paramagnetic contribution to the magnetic susceptibility, with a Curie constant at low field of $C = 0.966 \times 10^{-4}$ emu K g^{-1} or 4.6×10^{-3} emu K mol^{-1} for the present AlPdMn alloy (9.0 at.%)—see figure 2(b)—compared to $C = 1.6 \times 10^{-4}$ emu K g^{-1} for AlPdMn (9.6 at.%) [27]. For this latter composition we have detected a spin-glass ordering at $T_f = 1.1$ K, with an estimated concentration of Mn magnetic moments which is 1.4% of the total number of Mn atoms.

2.1.2. Al–Cu–Fe alloys. The samples came from a large-size polyquasicrystalline ingot prepared by conventional casting, and subsequent annealing at CECM (Vitry, France). The characterization and specific heat data were reported in a previous paper [28] (under the sample reference $Al_{63}Cu_{25}Fe_{12}$-b). The ingot was also icosahedral single phased, with a structural state close to the ideal quasiperiodic phase, and possible fluctuations of composition up to 0.5 at. % in the Fe or Cu, due to the large size of the sample. The resistivity data reported in figure 3 give $\rho_{300\,\mathrm{K}} = 2630\ \mu\Omega$ cm and a resistivity ratio $\rho_{4\,\mathrm{K}}/\rho_{300\,\mathrm{K}} = 1.82$, in excellent agreement with previous measurements on ingots of similarly high structural quality [29]. Note that, as in the case of AlPdRe, the resistivity value is very sensitive to the composition.

Specific heat measurements performed on this ingot, if analysed below about 2 K in a conventional manner as $C = \gamma T + \beta T^3$, yield an electronic coefficient $\gamma = 0.345$ mJ mol^{-1} K^{-2} and a lattice term $\beta = 0.011$ mJ mol^{-1} K^{-4}, which corresponds to

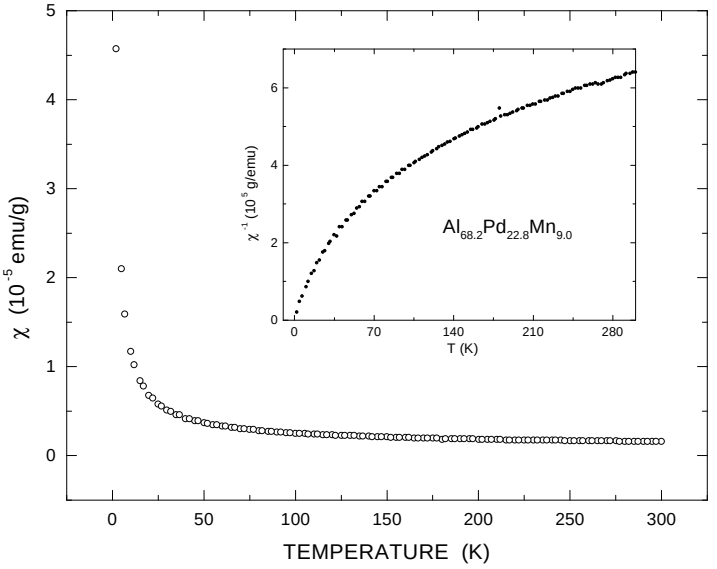

(*a*)

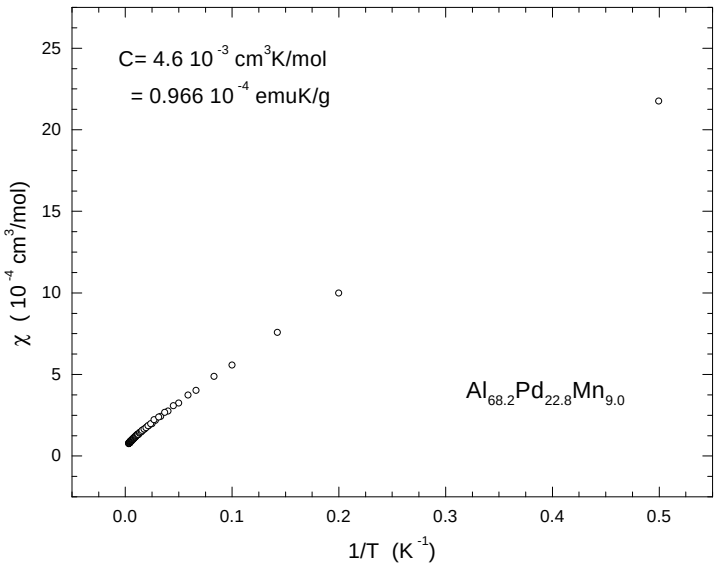

(*b*)

Figure 2. (*a*) The temperature dependence of the DC susceptibility for i-$Al_{68.2}Pd_{22.8}Mn_{9.0}$ in a field of 10^3 Oe. (*b*) Susceptibility versus $1/T$: the slope represents the Curie constant, with a value of 4.6×10^{-3} emu K mol^{-1} or 0.966×10^{-4} emu K g^{-1}.

a low-T-limit Debye temperature $\theta_D = 560$ K [28]. Both the γ- and β-values are in excellent agreement with the previously published ones determined for the same low T-range [10]. The high Debye temperature, defined only in the low-temperature limit, gives additional evidence for the quality of the QC phase. Magnetization measurements, performed on parts of the ingot, using sensitive SQUID techniques at the CRTBT-CNRS, could detect a small paramagnetic

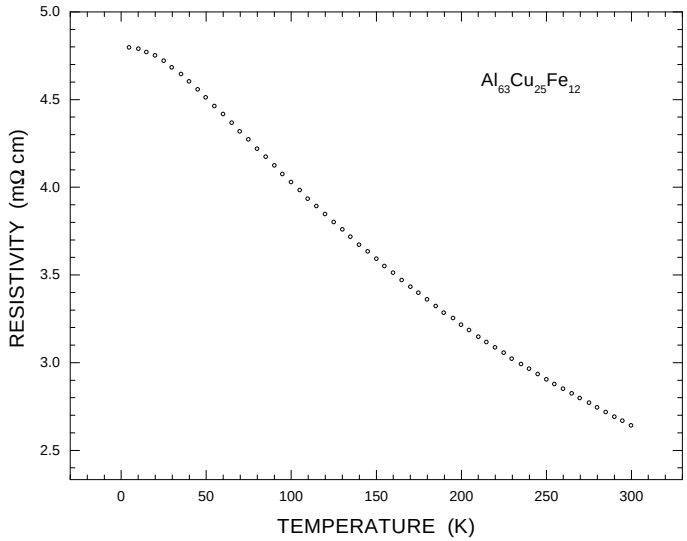

Figure 3. The temperature dependence of the resistivity for i-$Al_{63}Cu_{25}Fe_{12}$.

contribution in addition to the diamagnetic intrinsic one, which yields a fraction of 2×10^{-4} of the total number of Fe atoms which are magnetic (with spin $S = 2$).

2.1.3. Al–Pd–Re alloys. The Al–Pd–Re quasicrystals were also prepared at CECM-CNRS (Vitry, France). $Al_{70.5}Pd_{21}Re_{8.5}$ ingots were made from high-purity elements by induction melting, under helium atmosphere. The entire ingots were re-melted and rapidly quenched by planar flow-casting on a rotating copper wheel under helium. The flakes produced were annealed in a good vacuum at 900 °C for about six hours; it is worth mentioning that this last step of the preparation method is very important for relaxing strains and avoiding inhomogeneities. After this heat treatment, the x-ray diffraction spectrum from the powered samples consists of very sharp peaks *all of which* have been indexed using an F-type icosahedral quasicrystal. These measurements show that the samples are single phased, and of high structural quality. The characterizations of the electrical properties of the alloys were also performed by electrical resistance measurements between room temperature and 4 K. Figures 4(*a*) and 4(*b*) present typical behaviour, with ratios $R = R_{4\,\mathrm{K}}/R_{300\,\mathrm{K}}$ from 30 to 100 respectively (no attempt was made to evaluate the resistivity value, due mainly to the difficulty of estimating the geometrical factors of irregular pieces). In particular, we used the QCs shown in figure 4, to fabricate the junctions and to evaluate the width of the pseudogap, and these experiments will be described in the following sections. This value of the R-ratio is another indication of the quasicrystalline perfection of the alloy, and is in good agreement with other data from the literature, where the variations of the resistance ratio among different samples have also been noted [30]. Resistivity data from the literature indicate values at temperatures of 4 K which are of the order of 1 Ω cm, which are comparable to those for doped semiconductors. In contrast to this behaviour, the electronic γ-term of the specific heat remains typical of semi-metallic alloys, with values in the range 0.10 to 0.15 mJ mol^{-1} K^{-2} (see, for instance, references [11–14]). These results indicate that the large increase in resistivity, in comparison to that of Al–Cu–Fe, is not related to modifications of the band structure at E_F. This conclusion was also established from the unrelated variations of $\rho_{4\,\mathrm{K}}$ and γ among different Al–Pd–Re samples [14].

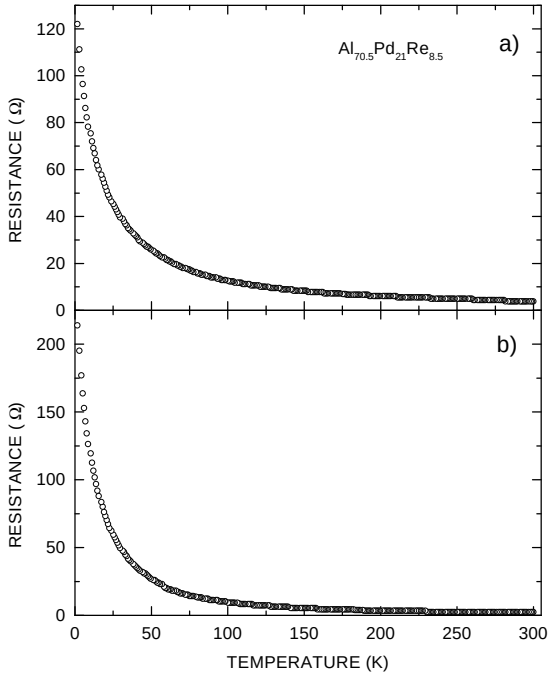

Figure 4. The temperature dependence of the resistance of two samples of i-$Al_{70.5}Pd_{21}Re_{8.5}$. The ratio of resistance $R = R_{4\,K}/R_{300\,K}$ is (*a*) 30 and (*b*) 100.

3. Tunnelling and point contact spectroscopy

The main study of the quasicrystalline alloys was performed using tunnel and point contact junctions. These junctions are formed in general when a sharp metallic tip touches a metal, or the alloy under study. The two techniques, tunnelling and point contact spectroscopy (PCS), have been used to probe gapping, nesting, and scattering processes, and excitations which occur in numerous systems in solid-state physics [31–36]. In addition, variations on the electronic density of states (DOS), such as non-constant DOS, can be studied [37]. This is in fact the main aim of this paper—to show that with these two techniques we can probe with very high resolution the pseudogap features developed in QC systems. With tunnelling spectroscopy we are able to probe in a direct manner the evidence of pseudogap features, and also the variations of the density of states, whereas with point contact spectroscopy we can, at least, observe—but in a different form—the features of the pseudogap. We should perhaps mention that in all former spectroscopic studies performed with PCS or tunnelling, it was always considered that the DOS was a constant without any variation. However, if this case arises, then the experimental information obtained from the tunnel junctions (as the differential resistance at zero bias) will represent a maximum, or the equivalent minimum in the differential conductance. This behaviour was shown in particular in early experiments performed on semiconducting systems by Bermon and So [38], and explained theoretically by Altshuler and Aronov [4].

From the theoretical point of view, this can be seen in the expression for the current $I(E)$

in the form [39]:

$$I(E) = A|T|^2 \int_{-\infty}^{\infty} N_{\mathrm{M}}(E) N_{\mathrm{alloy}}(E + eV)[f(E) - f(E + eV)]\,\mathrm{d}E. \qquad (1)$$

Here $|T|$ may be a constant matrix element that is very much dependent of the type of junction, while A is a constant related to the characteristics of the junction and barrier, and to the velocity of the electrons that pass through the constriction. The N_i are the densities of states of the two electrodes (metal and alloy) that form the junction. Within this simple framework of a semiconductor model, in general it is assumed that the independent-particle approximation for the densities of states $N_{\mathrm{M}}(E)$ and $N_{\mathrm{alloy}}(E)$ are constant near E_F. Nevertheless, it is reasonable to think that changes in, for instance, $N_{\mathrm{alloy}}(E)$ would influence the behaviour of $I(E)$, and these changes will be necessarily observed in the behaviour of the differential resistance $\mathrm{d}V/\mathrm{d}I$. Accordingly, dramatic changes will be seen if pseudogaps or minima in $N(E)$ develop. These changes, as a consequence, will lead to a maximum at zero bias voltage in $\mathrm{d}V/\mathrm{d}I$, and also to *peculiarities* in $\mathrm{d}V/\mathrm{d}I$. If the variations are slight or not very well defined, we can obtain the $\mathrm{d}^2V/\mathrm{d}I^2$ characteristic in order to improve the experimental resolution. It is worth mentioning that in past experiments performed by other workers on mixed-valence compounds, and on some metals and alloys with lanthanides, zero-bias anomalies (ZBA) were observed in the spectra of point contacts that were attributed to minima, gaps, or pseudogap features in the DOS [40–48]. Lastly, we must mention that we are considering here only elastic scattering processes, and that other excitations are not taken into account. Nevertheless, this simple model can give us a qualitative view of our experimental observations.

Tunnelling spectroscopy is a very precise spectroscopic technique, and it is very well known that is one of the most reliable and direct probes for studying the superconducting state—particularly the energy gap and the elementary excitations. But, as previously demonstrated, it can also be a very useful tool for studying other electronic processes and changes in the DOS that occur in semiconductor or metallic systems.

3.1. Junction preparation and characterization

In order to probe the pseudogap features of the QCs under study, we fabricated junctions with one of the electrodes being In, Au, or Al wire of high purity (99.999%) and diameter $\phi = 5\ \mu$m, the other electrode being the specimen to be studied. The junction configuration is the standard one: QC alloy–Au (In, Al). To form the junction, we take into account the native oxide that grows on the surface of the alloy. In other cases it was removed from the surface with an etching solution and the cleaned piece of QC was left in the air of the laboratory for different periods of time. The small diameter of the wires permits us to form junctions of very small area. The junctions are made by crossing the wire over the surface of the sample, taking care that the area of the contact is as small as possible. To obtain this small area of contact, we have to cut a piece of the alloy, leaving a sharp edge in such a form that when the wire crosses this part of the alloy it touches only one edge of the sample. The junctions fabricated in this form have dimensions which in general are smaller than $1 \times 1\ \mu\mathrm{m}^2$, as observed with a microscope. The junctions were measured at temperatures between 1.7 K and 40 or 70 K depending on the sample. We made measurements on about 20 junctions of each alloy, and checked that the results were reproducible. One of the important characteristics of this type of junction is the thermal stability—in contrast to what in general occurs in usual point contact junctions or STMs where, due to the thermal contractions that occur when the temperature changes, the part of the area of the crystal which is being sensed also changes [34, 49].

The measurements of the differential resistance, $\mathrm{d}V/\mathrm{d}I$, for both point contacts and tunnel junctions, were performed by using the conventional lock-in and modulation techniques [36].

Once we have collected all of the information on $\mathrm{d}V/\mathrm{d}I$ versus the bias voltage V at different temperatures, we can obtain the differential conductance by taking the inverse of the differential resistance.

4. Results and discussion

We have studied the devices over the range of temperatures from around 77 K down to 2 K, and even in the case of AlCuFe to 0.4 K. We observed a dramatic reduction of the density of states close to the Fermi energy. This anomaly in the density of states may be identified as a pseudogap. This pseudogap is not very well defined at high temperatures, but is very clearly defined at lower temperatures. In the many different junctions built to study this feature, we observed that the width of the pseudogap remains more or less constant when the temperature is changed, but is smeared out by $k_B T$. However, we observed that the depth of the anomaly changes and increases as the temperature decreases; the width remains constant but the DOS begins to become spiked, mainly at the Fermi level.

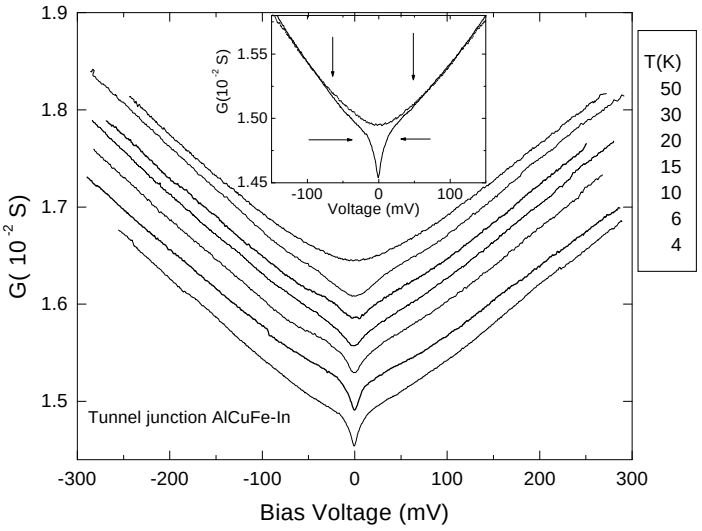

Figure 5. The differential conductance $G(V)$ as a function of the bias voltage for a tunnel junction of AlCuFe and indium at different temperatures between 50 and 4 K. Note in the central part of the curve the presence of the pseudogap. For clarity, the curves have been displaced vertically by constant amounts. The inset shows in detail the difference between the data at 50 and 4 K; the arrows indicate the size of the narrow feature and the broad pseudogap.

The width of the pseudogap (or spiky feature) can be defined as is indicated by the arrows on the tunnelling spectrum curves shown in the various figures. We can see for instance, as one example, the arrows defining the spiky feature and the size of the pseudogap in figure 5.

4.1. AlCuFe junctions

Differential conductance ($G(V) = \mathrm{d}I/\mathrm{d}V$) versus V characteristics for tunnel junctions of AlCuFe–In, AlCuFe–Au, and AlCuFe–Al of the above-mentioned compositions show similar and very symmetric characteristics. The thermal stability of the junctions allowed us to perform measurements from 50 K to 2 K, and even to 400 mK. A typical set of characteristics for a tunnel junction of AlCuFe–In are displayed in figure 5; the curves have been displaced vertically by

constant amounts, for clarity. It seems that a central feature is developing as the temperature decreases. The parabolic background changes in the central part, and starts to show a ZBA at a temperature of around 30 K. At lower temperatures the feature is well defined and becomes very evident from temperatures starting at 20 K and below. In the inset of the same figure we show the variation of the ZBA as compared with the curve at 50 K; the arrows show the spike feature and the broad pseudogap. This definition of the narrow pseudogap (as indicated by the arrow heads) is taken at the inflection of the curve, whereas the broad feature is taken to be when the two curves start to separate at high voltages. This figure and the inset show the size of the anomaly at low voltages as determined when the two curves start to separate (roughly) at around -47 meV, and $\sim +37$ meV. This inspection reveals that the width is about 84 meV. The width of the ZBA in the peaked central portion of the curves fluctuates between 20 meV and 22 meV, as determined for different junctions.

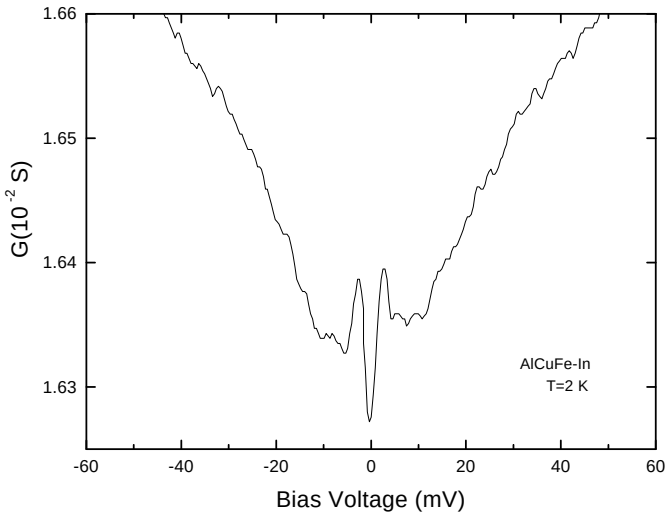

Figure 6. The differential conductance for the tunnel junction of figure 5 at a temperature of 2 K. The curve shows the superconducting energy gap of In.

In order to be completely sure that the data that we are observing are the tunnelling characteristics, it is important to check the spectrum of the junction with a superconducting electrode to see the development of the energy gap feature of the superconductor. In order to do this, we used a tunnel junction with one superconducting electrode. The indium electrode becomes superconducting at about 3.4 K. In figure 6 we clearly see the superconducting gap feature which appears when the temperature goes down below the superconducting transition temperature. It is very important to mention that in fact this is really the only reliable method of verification for a tunnel junction and that the characteristic of the differential conductance versus bias voltage is indeed due to tunnelling currents. This check was carried out for all of the measurements reported in this work using superconducting electrodes. Following our analysis, in figure 7 we show the variation with temperature of the differential conductance normalized to the value at 50 K; we can see in this plot the decrease of the density of states around the Fermi energy due to the opening of the pseudogap feature at low T. Clearly this figure shows that the pseudogap is developing and the DOS is being reduced.

In figure 8, we show another tunnelling spectrum of the $Al_{63}Cu_{25}Fe_{12}$–Al taken at $T = 2$ K; we observe the characteristic feature of the pseudogap in the central portion of the curve. As

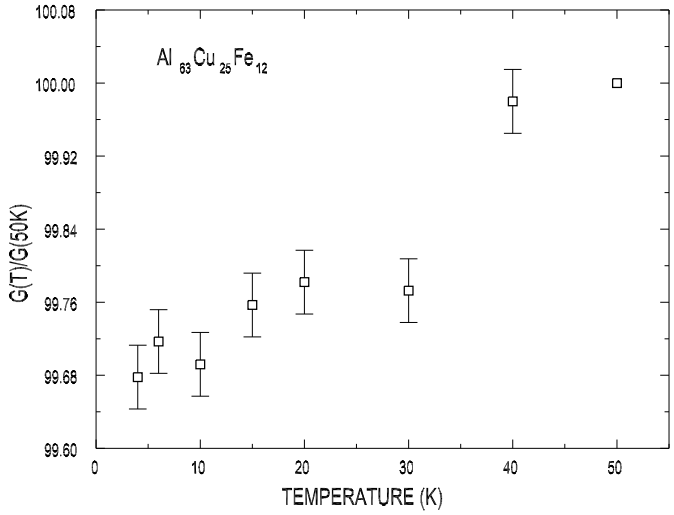

Figure 7. $G(T)/G(50\ \mathrm{K})$ versus temperature for the tunnel junction of AlCuFe–In of figure 5; this shows the reduction of the density of states, from 50 to 4 K, due to the occurrence of the pseudogap.

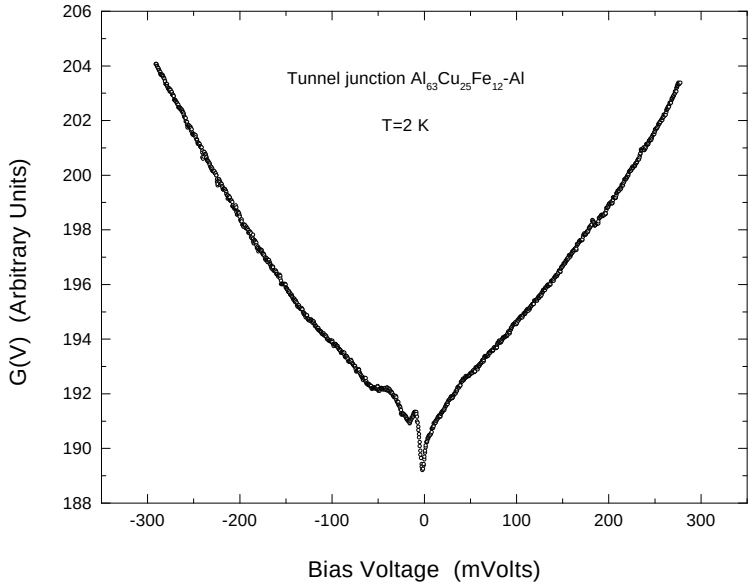

Figure 8. The differential conductance for an AlCuFe–Al tunnel junction at a temperature of 2 K. The characteristic shows an asymmetric structure on only one side of the curve.

mentioned before, the small area of the junctions permits investigation of local variations, and thus the local depression in the DOS. It seems that a fine structure appears in different parts of the sample. It is important to mention that our very small junctions sometimes show very fine structures. A reasonable explanation for this is that in the tunnelling area of these samples there may be portions of material with a better structural quasicrystalline quality than other parts of the QC. Due to the small size of the junction, producing a complete evolution with temperature

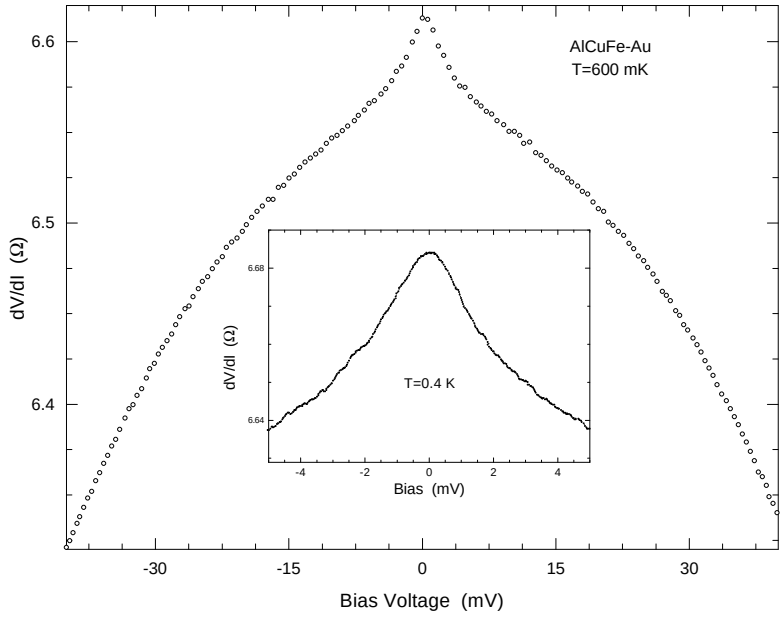

Figure 9. The differential resistance versus the bias voltage for an AlCuFe–Au junction at 0.6 K, and 0.4 K (inset). The data were taken with a very small modulating voltage and at low temperature, in order to minimize the thermal and instrumental smearing.

becomes a very difficult task, because thermal contractions move the area which is sensed by the junction. In figure 8 we see a spiky feature followed by an asymmetric structure similar, in some ways, to the DOS spectra predicted by Fujiwara and Yokokawa [6,7]. Lastly, for AlCuFe junctions other than those represented in figure 7, more information was obtained at still lower temperatures, as shown in figure 9, down to about 600 mK. In this figure it seems that the feature of the pseudogap persists, but without any additional fine substructural peaks. At this lower temperature the modulation voltage was kept as small as the thermal noise, in order to allow observation of the data with the minimum thermal or modulating voltage broadening. The characteristic shows the same background, and no traces of further fine structure in the spectrum. In this figure the inset shows the central part of the peak at 400 mK, with no additional features appearing.

4.2. AlPdMn junctions

Figure 10 shows the differential conductance versus the bias voltage for a set of typical data for a tunnel junction at different temperatures, obtained for a junction of AlPdMn–Au. For clarity the curves were vertically displaced by constant amounts. The most notable feature in these figures is the central peak at zero bias voltage (the so called ZBA). The width of this pseudogap feature is about 17–20 meV, which represents the averaged spread obtained over 20 junctions. These values have been obtained by taking measurements of the width which is defined by the arrows on each side of the ZBA. The changes of width can be ascribed to inhomogeneities of the alloy in different parts of the specimen measured.

The next feature worth observing is related to the smearing of the peak as temperature increases. In figure 10 we note that at low temperatures the central peak is clearly defined, but it disappears with increasing temperature. The inset of this figure shows a closer view of the

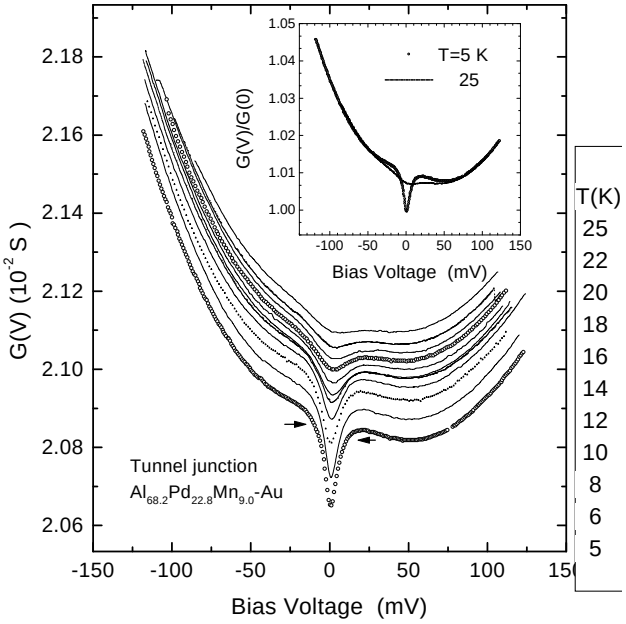

Figure 10. The differential conductance for a tunnel junction of AlPdMn–Au, at temperatures from 25 K to 5 K. The characteristics are identical at high bias voltages. Note the clear distortion of the curve at low temperature indicating the presence of the pseudogap. The inset shows the modification of the differential conductance at 25 and 2 K due to the presence of the pseudogap.

two curves taken at 5 and 25 K; here the vertical axis represents the normalized differential conductance. Closer inspection reveals that the anomaly starts (roughly) at around −45 meV, going to about +68 meV, so the width of this feature is about 113 meV. The spiked feature is as narrow as about 17–20 meV centred at the Fermi level. It is interesting to observe that a deformation emerges in the density of states in the parabolic background on both sides of the ZBA.

This dependence of the zero-bias anomaly on temperature must necessarily be due to variations in the electronic interaction strength that lead to an enhancement of the cohesive energy. This interaction, according to our experiments, strengthens with the reduction of temperature. Figure 11 shows the evolution of the anomaly, plotted as the differential conductance normalized with respect to the differential conductance at 25 K, which is the conductance at which the pseudogap starts to be defined (of course, the feature seems to appear at higher temperature according to the experiments, but can be neglected for temperatures higher than ∼40 K). The decrease of the normalized conductance as the temperature decreases means that the DOS is decreasing in comparison to the DOS taken at 25 K, due to the reinforcing of the pseudogap feature.

A very important test to check the behaviour of our junctions in order to probe whether this ZBA is due to the reduction of the DOS in the alloy, and not to other effects intrinsic to the junction itself or to the magnetic behaviour of the alloy, is the test of the character of the ZBA made by observing its behaviour in the presence of high magnetic fields. We have performed measurements in magnetic fields as high as 5 T. Our experiments show that the ZBA is not due to magnetic effects—for example, a type of Appelbaum ZBA frequently observed in tunnel junctions when the electrodes that form the junction have a magnetic character [36, 50, 51].

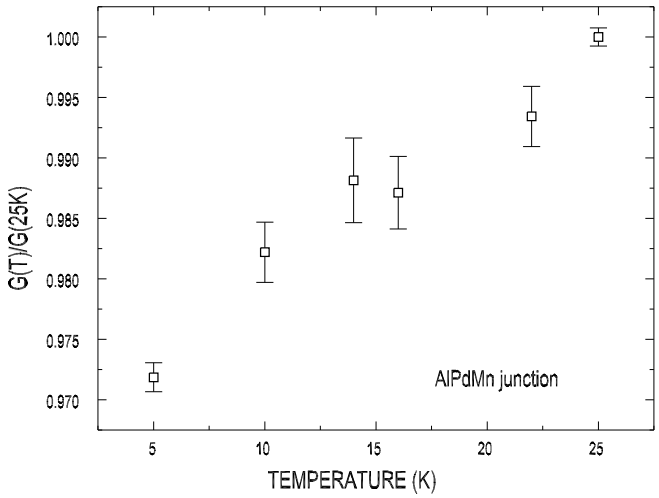

Figure 11. Normalized conductances $G(T)/G(25\ \mathrm{K})$ as a function of temperature for the tunnel junction of AlPdMn–Au of figure 10, showing the depression of the density of states due to the presence and evolution of the pseudogap.

For these junctions and using these data, we determine a pseudogap feature centred at around the Fermi energy, with widths between 17 and 20 meV, but revealing the deformation of the DOS at energies of width around 110–122 meV, and without any additional fine structure.

4.3. AlPdRe junctions

In figure 12 we present data for a point contact junction formed with AlPdRe–Au measured at temperatures from 70 K to about 2 K. The electrical resistance of the QC studied in these junctions was measured and is shown in figure 4(*a*); the QC has a resistance ratio $R = R_{4\,\mathrm{K}}/R_{300\,\mathrm{K}} = 30$. We observe a dramatic evolution of the ZBA in the differential resistance versus voltage characteristic. In this figure the change suffered by the ZBA when the temperature is reduced to about 2 K reaches an extraordinarily high value, increasing in value from about 50 Ω at 70 K to about 500 Ω at 2 K. Another feature can easily be seen in the curves, mainly at lower T: for instance at 2 K we can detect a change at about ±340 mV (as marked by arrows).

More information related to the data of figure 12 can be seen in figure 13, where we have plotted the differential conductance for just two curves, at 2 K and 50 K. To emphasize the effect of the temperature on the pseudogap feature, the curves were displaced to superpose on each other and so to emphasize the differences between them. Note that at 50 K the behaviour is parabolic, without any additional structure, whereas at 2 K a ZBA deviation occurs at zero voltage; also note that the feature observed in figure 12, as an inflection at about ±340 mV, can be seen in the differential conductance as a very slight peculiarity at the same voltage, but now enhanced because of the difference between the parabolic behaviour at high temperature and the non-parabolic behaviour at 2 K. In the inset of this figure we see clearly the ZBA at 2 K, with a width of the order of 120 mV.

Figure 14 shows the characteristic of a tunnel junction made with the QC of figure 4(*b*), which has a resistance ratio $R = 100$. Here, as in other tunnel junctions, the second electrode was Au. The oxide used to form the barrier of the junction was the oxide formed by, first,

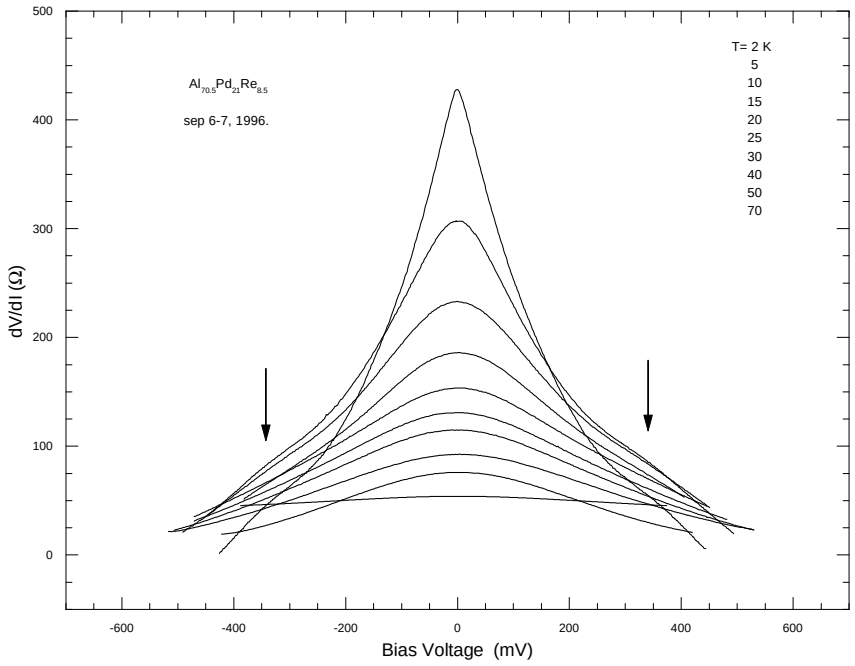

Figure 12. The differential resistance for a point contact junction of AlPdRe–Au at different temperatures from 70 to 2 K; the AlPdRe quasicrystal has a resistance ratio of $R = 30$. Note the dramatic increase of the ZBA on decreasing the temperature.

cleaning the native oxide of the surface of the QC, and, secondly, leaving the sample exposed for a period of time to the laboratory atmosphere.

In this tunnel junction we can see, as in the point contact junction of figures 12 and 13, a similar dramatic change of the ZBA between 2 K and 70 K, but now the peak is larger and more spiky. In this junction the differential resistance at 70 K is close to 3300 Ω, measured at the top of the peak of the ZBA, the intensity of the anomaly being of the order of 400 Ω, defined from zero voltage to about ±100 mV. The large increases of the ZBA at 2 K were observed to be about 3000 Ω measured from the background of the ZBA, the value of which is of the order of 1800 Ω at −600 mV, to the cusp which is close to 6000 Ω (note that the set of curves in figure 14 were displaced vertically by constant amounts, 1000 Ω). Figure 15 shows the width of the ZBA as determined by the horizontal arrows on the curve: this is about 105 mV.

The width of the pseudogap determined in nine junctions with resistance ratios R of around 100 varies around 100–110 meV. The interesting observation is that the ZBA (i.e. the spiky pseudogap) *tends to become narrower as the resistance ratio R increases*, whereas for junctions with resistance ratios of the order of $R = 30$ the spiky feature is more attenuated, as was shown in figure 13. It is important to mention that in contrast to what occurs in junctions prepared with other QC alloys, we consistently observed that the ZBA persisted at high temperatures (at about 70 K) when the ratio of the resistances R was of the order of 100. This contrasting behaviour, with respect to that of other QC alloys, could be a clear indication that the effects of the Coulomb interactions are stronger in those QCs than in others.

In relation to these tunnelling measurements, it is important to remember that in tunnelling experiments related to the study of the electronic localization, where it has been postulated that the ZBA is the signature of the correlation gap, the tunnelling data are quite similar

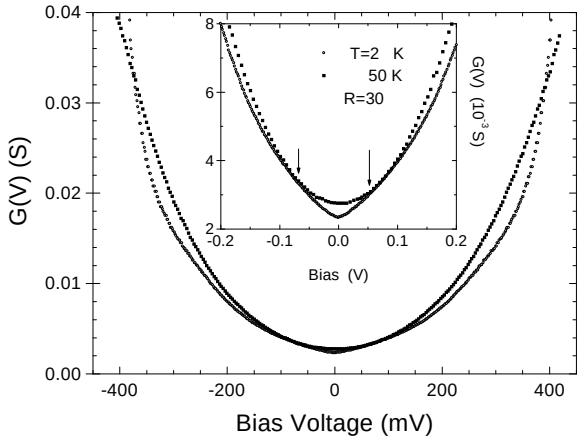

Figure 13. Differential conductances for the same junction as in figure 12, at 2 and 50 K, superimposed to show the differences due to the pseudogap at low temperature. Note the deviation from the parabolic shape in the curve at 2 K mainly in the central portion of the curve. The inset shows the detail of the ZBA anomaly and the departure from the parabolic shape at high voltages in the curve measured at 2 K, by comparison to the curve at 50 K.

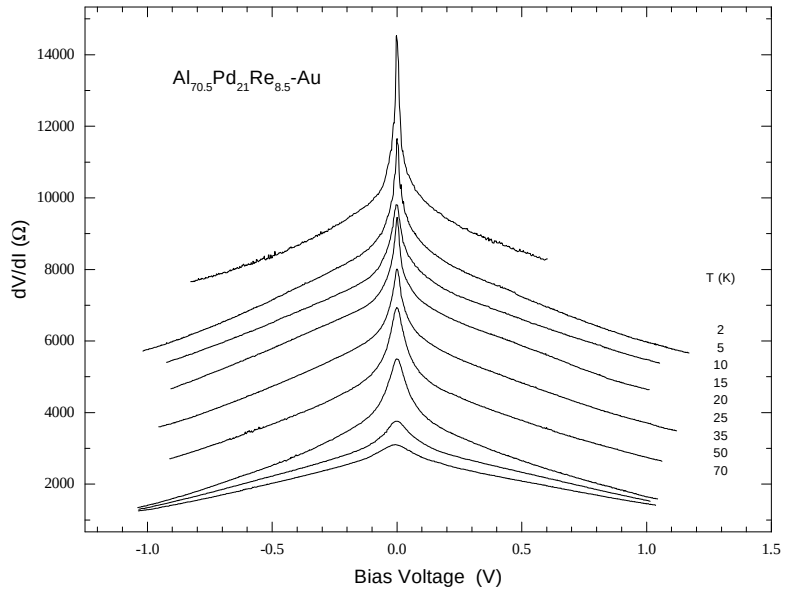

Figure 14. The differential resistance characteristic for a tunnel junction made with a quasicrystal of AlPdRe with a resistance ratio of $R = 100$. The curves are displaced vertically to show the growing of the ZBA. Note also the sharpness of the peak.

to our experimental data. McMillan, White, Schmitz, Meekes and co-workers [40, 52–54] have shown such a behaviour in studies performed on amorphous films, granular systems, and chromium single crystals. For the former, a correlation gap is at the origin of the ZBA, whereas for the latter the origin is the opening of a gap due to nesting of parts of the Fermi surface. To obtain a better idea of the modification of the DOS by the electronic interactions in this QC,

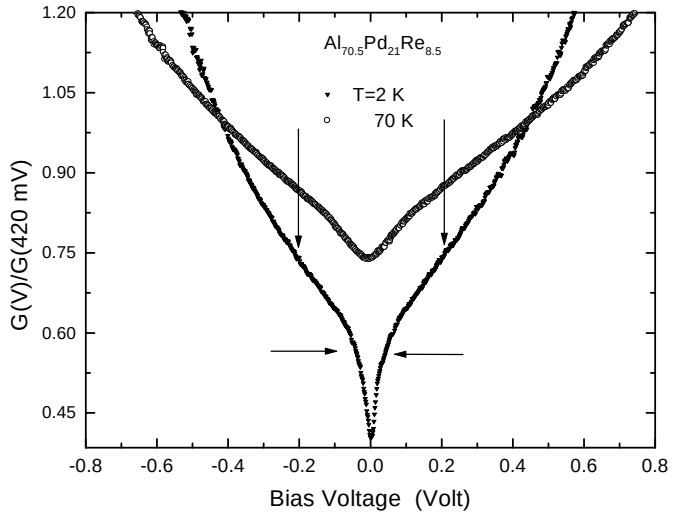

Figure 15. The differential conductance normalized at 420 meV of a tunnel junction made with AlPdRe–Au, the resistance ratio of the QC being $R = 100$. One can see clearly in the curves the modification introduced by the presence of the pseudogap at 70 and 2 K; the widths of the features are marked by arrows.

we have plotted in figure 15 the differential conductance $G(V)$ normalized with respect to the 420 meV differential conductance, $G(420)$ (the normalized energy being arbitrary). At this point it is important to remember that in tunnelling experiments at low temperatures, $G(V)$ is proportional to the density of states $N(E)$. Therefore, in view of the enormous change observed in this figure, we assert that there is a strong modification of the DOS when the QC is cooled to low temperatures. The larger reduction is observed close to the Fermi energy; the width of the peak (the ZBA) defined by the horizontal arrows in the figure is about 105 meV, but a wider depression is also observed, from about -0.2 V to 0.2 V (marked by long vertical arrows), this broader and large pseudogap being about 400 ± 40 meV.

It has been noted in theoretical studies of disordered systems that the Coulomb interaction has the consequence of reducing the DOS around the Fermi level, leading to a square-root or logarithmic energy dependence of the DOS [4, 5, 52], and consequently of changing many of the electronic properties of the systems—for example, turning the system into an insulator. The depression of the DOS around the Fermi energy, or, in other words, the development of this pseudogap feature, has been observed in many different disordered alloys by using different experimental probes. In particular, electron tunnelling spectroscopy was used to study this effect, and it shows, as experimental corroboration of the existence of a pseudogap feature in the DOS, a ZBA which becomes sharper as temperature decreases [38, 52, 54–57].

However, in the case of the QC alloys, which can be considered as non-periodic but ordered structures, in fact there are no theoretical models that can be directly applied to interpret the experimental observations, i.e. from experiments using electron tunnelling or point contact junctions—contrary to the case for the disordered or amorphous alloys in recent years.

One of the most important problems to solve in the studies of QC alloys, and directly related to the interpretation of experiments which use junction devices, is related to the lack of observation of the spiky features in the DOS which were predicted by theoretical arguments [2, 7]. The lack of visible spiky structure, which is a very controversial problem, can be attributed in particular to some residual disorder character of QCs, present even in

samples of high structural quality, as proved by different physical properties (such as the presence of two-level states, as in glasses), and which could smear out the fine structure of the DOS (see, e.g., reference [24]).

In spite of this lack of theoretical models appropriate for the interpretation of experiments performed on tunnel or PCS junctions, two models which might be relevant for the analysis and interpretation of the data have been proposed for deducing the widths of pseudogap features and modifications in the DOS which occur in QC alloys. Here, in this work, we compare our results to the scaling theory proposed by McMillan and Mochel [52], and the theory of Altshuler *et al* [4, 5]. Nevertheless, we have to stress that these models are appropriate to the study of amorphous and disordered materials, not really QC alloys.

To look forward in the description and meaning of the experiments performed using junctions, it is important to remember that in tunnelling or PCS experiments the differential conductance versus voltage data are directly related to the DOS when it is measured at low temperatures. Thus, the experiments performed with junctions will provide information about how the DOS is changed by the effects of the temperature and the electronic interactions.

In the first model, McMillan incorporates three physical processes: localization, screening, and correlation effects. Correlation effects in this model are included by adapting a weak-coupling approximation given by Altshuler and Aronov, and Altshuler *et al* [5, 58]. As a result, the McMillan prediction is that a singularity must appear in the single-particle density of states at the Fermi level $N(0)$ leading, as temperature goes to zero, to localization in the system, and consequently the formation of a correlation gap. The change in DOS predicted by this theory follows the equation

$$N(E) = N(0)[1 + (E/\Delta)^{1/2}]. \tag{2}$$

Here, in this equation, Δ is the correlation gap and E is the energy. The experimental observation of the behaviour of $N(E)$ gives rise to a cusp-like peak at $V = 0$ in the tunnelling differential resistance, or to a cusp-like depression in the differential conductance, which is the so-called ZBA. The model fits well to the present experimental data, and can be easily applied because the only fitting parameter is the value of the correlation gap Δ. The second model relating to weakly disordered metals that leads to localization and to a correction to the DOS near the Fermi level was proposed by Altshuler and Aronov [4, 5]. In this model the influence of the electron–electron scattering and impurities causes a depression in the DOS near the Fermi level. The DOS in this case is given by the equation

$$\frac{\delta N(E)}{N(0)} = \frac{\lambda}{2\sqrt{2}\pi^2(\overline{h}D)^{3/2}N(0)}\sqrt{E} \tag{3}$$

which in an abbreviated form we write as

$$\frac{\delta N(E)}{N(0)} = m\sqrt{E}. \tag{4}$$

Here, in the equation, λ is the electron–electron interaction factor, D is the diffusion coefficient due to the impurity scattering, and $N(0)$ is the DOS at the Fermi level. As Altshuler and Aronov explain, this singularity in the density of states leads to the zero-bias anomaly that can be observed in tunnelling experiments.

In figures 16 and 17 we display the experimental data plotted as the normalized conductance versus the bias voltage. This behaviour illustrates that the experimental data follow both models reasonably well. In both figures the fitting of the Altshuler–Aronov model was made including a normalization to 1, with the idea of fitting both theoretical models in the same figure and in that form observing the coincidence of the two models with the experimental data. In figure 16 for AlPdRe the value of Δ, the McMillan parameter, which gives the best fit

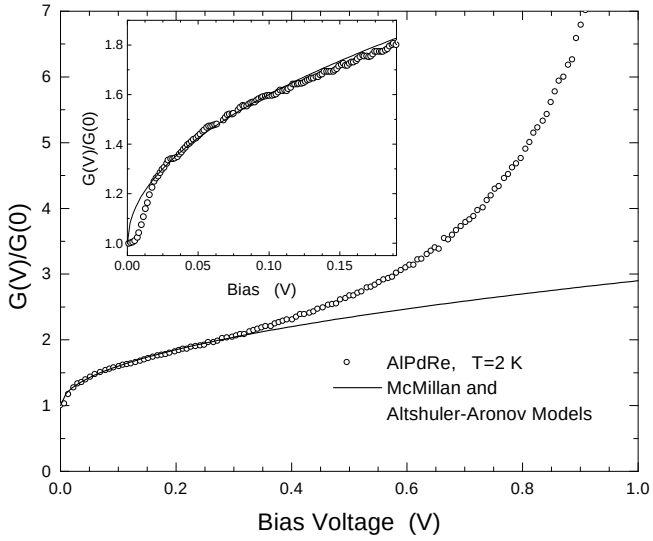

Figure 16. The normalized differential conductance of the junction of AlPdRe at 2 K shown in figure 15 and the fit to the McMillan and Altshuler–Aronov models. Δ, the correlation gap, was in this case estimated to be about 270 meV, whereas the parameter m was about 1.9. Note, in the inset, the discrepancy at low energies between the data and the theoretical models.

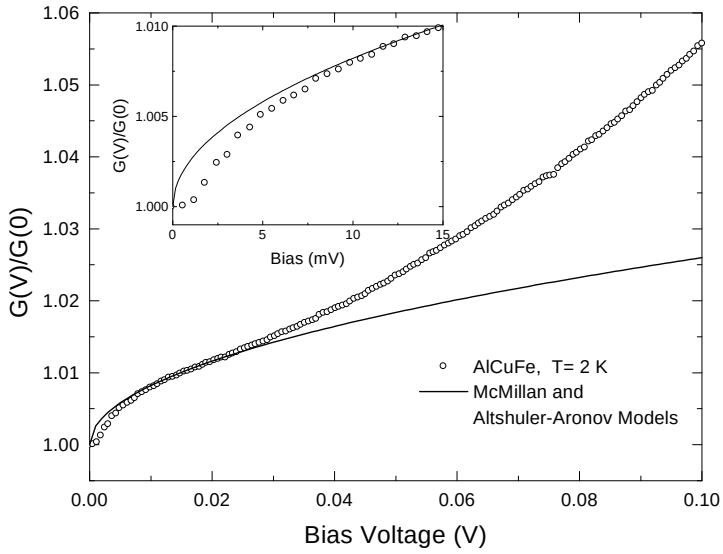

Figure 17. The normalized differential conductance of the junction of AlCuFe at 2 K shown in figure 10; the continuous curve shows the McMillan and Altshuler–Aronov models. The parameter Δ in the McMillan model is 148 meV, whereas m in the second model is 0.082. This latter value of the parameter seems unphysical. As in figure 16, note in the inset the discrepancy between the data and the theoretical models at low energies.

was estimated to be about 270 meV, whereas the coefficient m for the Altshuler–Aronov model is about 1.9, which is correct and in agreement with numerical coefficients for the AlPdRe alloy. The theoretical models agree reasonably well with the experimental data up to about 300 meV.

At low energies (from 0 to 30 meV) the discrepancy is larger, and this difference reflects the sharp feature in the gap structure close to the Fermi level which could be related to the expected spiky behaviour of the DOS on a scale of 10 meV or less [6, 7]. This clear discrepancy at low voltages can be observed in the insets of figure 16 and figure 17. Obviously, this extra feature was not considered in the McMillan and Altshuler–Aronov theoretical models. Figure 17 shows the results of the best fits to our experimental data using the two models for AlCuFe QC data measured at 2 K. In this case the value determined for the Δ parameter is about 148 meV, whereas $m = 0.082$. This latter fitting value for the m-parameter looks unphysical, and is quite small for the alloy under consideration (see Klein *et al* [19]). Nevertheless, the models fit reasonably well to the experimental data, mainly at energies of the order of 30 meV and above. However, again at low energies, as seen in figure 16, the fit is far from the experimental data. We believe that the same explanation can be applied as for the AlPdRe QC of figure 16: a specific theory for explaining tunnelling or point contact spectroscopy experiments on QC systems has not yet been developed. For the case of the AlPdMn QC, we could not fit the data to either of the two models, even by trying to use unphysical values for the parameters Δ and m. So, again the explanation looks simple: both models are applicable for explaining a metal–insulator transition, and in particular AlPdMn does not show any tendency to become insulating at low temperatures.

Lastly, we can observe that in both figures 16 and 17 the theoretical models are no longer valid at high bias (although the high biases in the two figures differ by an order of magnitude). We believe that the different ranges of fitting in energy for distinct QCs has to be related to the range of modification that occurs in the DOS, and depends on the intensity of the strength of the interaction in regions close to the Fermi energy. In spite of the former observation that neither model is really appropriate for explaining the physical behaviour related to the DOS features close to the Fermi level of the QCs, they give a plausible qualitative explanation of modifications of the DOS that in general look to be in good agreement with the broad pseudogap measurements obtained for our junctions. The fitting of the two theoretical models to our data in general gives reproducible results for different junctions, like for those reported on in the figures 16 and 17, with only about 10–15% variations of the parameters Δ and m. We note that a similar spread was observed in our measurements of the broad pseudogap and spiky features. These results are different from those obtained by Davydov *et al* [20], who observed a spreading of about 50% among different tunnelling junctions.

5. Conclusions

We have performed a number of tunnelling and point contact experiments at low temperatures on high-quality QC samples of AlCuFe, AlPdMn, and AlPdRe. The results are reproducible and show a ZBA peak in the differential resistance versus bias voltage characteristic, which is indicative of a pseudogap in the electronic density of states at the Fermi level. A general conclusion from our experiments is that the structure of the DOS reveals a small spiky gap of width of the order of few tens of meV, superimposed on a broad pseudogap. We have observed that the behaviour of the AlPdRe QC is different from those of the other two QCs studied. The difference consists mainly in the fact that AlPdRe has a significantly lower DOS and a larger pseudogap. The values of these pseudogaps in the different QCs show widths from 20 to 22 meV and broad changes of about 80–90 meV for AlCuFe, widths from about 17 to 20 meV and broad backgrounds of about 110–122 meV for AlPdMn, and for the AlPdRe system wider variations, around 100–110 meV, and broad features with widths as big as 400 meV. We observed that the ZBA becomes smeared out when the temperature increases. This trend of reduction of the ZBA is different for the three different QCs studied, and this can

be taken as an indication of the different strengths of the electron–electron interaction in these different QCs. In particular, in the AlPdRe alloy the anomaly related to the pseudogap is still clearly observed at temperatures as high as 70 K. We have observed in the case of the AlPdRe QCs that the features related to the pseudogap and to the spiky feature strongly depend on the resistance ratio, which is known to be very sensitive to the structural quality and to slight compositional variations [11, 30]. We have verified that for only two of the QCs (AlPdRe and AlCuFe) was it possible to fit our data to the McMillan and Altshuler–Aronov theoretical models; one possible explanation is that the AlPdMn alloy is conducting at low temperatures whereas the other two tend to be insulating, and both models were thought to provide plausible explanations for the metal–insulator transition in disordered materials. We also observe that the fitting of the experimental data to both models is good over a certain bias voltage range, but that a discrepancy exists at very low voltages, below around 10 meV. Again we think that the reason is that the two models are more or less appropriate for explaining the overall changes in the DOS in QCs, but not the spiky features predicted to occur from more *ad hoc* theories.

Lastly, as a further step to improve our understanding of the electronic properties of QCs, particularly concerning the modifications which occur in the DOS close to the Fermi energy, future experiments must be performed on materials of the best structural quality, controlled as in the case of AlPdRe by the highest possible resistivity ratio.

Acknowledgments

We are grateful for enlightening discussions with F Morales, P Monceau, and A Briggs. This work was partially supported by grants from the Organization of American States, by the Dirección General de Apoyos al Personal Académico of the Universidad Nacional Autónoma de México, grant: IN105597, and by the Consejo Nacional de Ciencia y Tecnología of México, grant: 400359-5-G0017E.

References

[1] *Proc. ICQ-4: 4th Int. Conf. on Quasicrystals (St Louis, 1992), J. Non-Cryst. Solids* 1993 **153+154**
Janot C and Mosseri R (ed) 1995 *Proc. ICQ-5: 5th Int. Conf. on Quasicrystals* (Singapore: World Scientific)
[2] Fujiwara T, Yamamoto S and Trambly de Laissardière G 1993 *Phys. Rev. Lett.* **71** 4166
[3] Fujiwara T, Mitsui T, Yamamoto S and Trambly de Laissardière G 1995 *Proc. ICQ-5: 5th Int. Conf. on Quasicrystals* ed C Janot and R Mosseri (Singapore: World Scientific) p 393
[4] Altshuler B L and Aronov A G 1979 *Solid State Commun.* **30** 115
[5] Altshuler B L, Aronov A G and Lee P A 1980 *Phys. Rev. Lett.* **44** 1288
[6] Fujiwara T 1989 *Phys. Rev.* B **40** 942
[7] Fujiwara T and Yokokawa T 1991 *Phys. Rev. Lett.* **66** 333
[8] Friedel J and Dénoyer F 1987 *C. R. Acad. Sci., Paris* II **305** 171
[9] Klein T, Berger C, Mayou D and Cyrot-Lackmann F 1991 *Phys. Rev. Lett.* **66** 2907
[10] Pierce F S, Bancel P A, Biggs B D, Guo Q and Poon S J 1993 *Phys. Rev.* B **47** 5670
[11] Berger C *et al* 1996 *Proc. 9th Int. Conf. on Rapidly Quenched Metals (Bratislava)*
Delahaye J, Gignoux C, Schaub T, Berger C, Grenet T, Sulpice A, Préjean J J and Lasjaunias J C 1998 *Proc 10th Int. Conf. on Liquid and Amorphous Metals (Germany)*
[12] Préjean J J, Lasjaunias J C, Berger C and Sulpice A 1999 to be published
[13] Chernikov M A, Bianchi A, Felder E, Gubler U and Ott H R 1996 *Europhys. Lett.* **35** 431
[14] Pierce F S, Guo Q and Poon S J 1994 *Phys. Rev. Lett.* **73** 2220
[15] Mori M, Matsuo S, Ishimasa T, Matsuura T, Kamiya K, Inokuchi H and Matsukawa T 1991 *J. Phys.: Condens. Matter* **3** 767
[16] Zhang G W, Stadnik Z M, Tsai A P and Inoue A 1994 *Phys. Rev.* B **50** 6696
[17] Belin E, Dankhazi Z, Sadoc A, Calvayrac Y, Klein T and Dubois J M 1992 *J. Phys.: Condens. Matter* **4** 4459

[18] Belin E, Dankhazi Z, Sadoc A, Flank A M, Poon J S, Müller H and Kirchmayr H 1995 *Proc. ICQ-5: 5th Int. Conf. on Quasicrystals* ed C Janot and R Mosseri (Singapore: World Scientific) p 435
[19] Klein T, Symko O G, Davydov D N and Jansen A G M 1995 *Phys. Rev. Lett.* **74** 3656
[20] Davydov D N, Mayou D, Berger C, Gignoux C, Neumann A, Jansen A G M and Wyder P 1996 *Phys. Rev. Lett.* **77** 3173
[21] Gignoux C, Berger C, Fourcaudot G, Grieco J C and Cyrot-Lackmann F 1995 *Proc. ICQ-5: 5th Int. Conf. on Quasicrystals* ed C Janot and R Mosseri (Singapore: World Scientific) p 452
[22] Belin E, Dankhazi Z and Sadoc A 1994 *Mater. Sci. Eng.* A **181+182** 717
[23] Wu X, Kycia S W, Olson C G, Benning P J, Goldman A I and Lynch D W 1995 *Phys. Rev. Lett.* **75** 4540
[24] Stadnik Z M, Purdie D, Garnier M, Baer Y, Tsai A-P, Inoue A, Edagawa K, Takeuchi S 1996 *Phys. Rev. Lett.* **77** 1777
Stadnik Z M, Purdie D, Garnier M, Baer Y, Tsai A-P, Inoue A, Edagawa K, Takeuchi S and Buschow K H J 1997 *Phys. Rev.* B **55** 10 938
[25] Boudard M, Bourgeat-Lami E, de Boissieu M, Janot C, Durand-Charre M, Klein H, Audier M and Hennion B 1995 *Phil. Mag. Lett.* **71** 11
[26] Lanco P, Klein T, Berger C, Cyrot-Lackmann F, Fourcaudot G and Sulpice A 1992 *Europhys. Lett.* **18** 227
[27] Lasjaunias J C, Sulpice A, Keller N, Prejéan J J and de Boissieu M 1995 *Phys. Rev.* B **52** 886
[28] Lasjaunias J C, Calvayrac Y and Yang H 1997 *J. Physique* I **7** 959
[29] Klein T, Gozlan A, Berger C, Cyrot-Lackmann F, Calvayrac Y, Quivy A and Fillion G 1990 *Europhys. Lett.* **13** 129
Klein T, Gozlan A, Berger C, Cyrot-Lackmann F, Calvayrac Y, Quivy A and Fillion G 1990 *J. Non-Cryst. Solids.* **165+166** 283
[30] Berger C, Grenet T, Lindqvist P, Lanco P, Grieco J C, Fourcaudot G and Cyrot-Lackmann F 1993 *Solid State Commun.* **87** 977
[31] Jansen A G M, van Gelder A P and Wyder P 1980 *J. Phys. C: Solid State Phys.* **13** 6073
[32] Yanson I K and Shklyarevskii O I 1986 *Sov. J. Low Temp. Phys.* **12** 509
[33] Blonder G E, Tinkham M and Klapwijk T M 1982 *Phys. Rev.* B **25** 4515
[34] Escudero R, Morales F and Lejay P 1994 *Phys. Rev.* B **49** 15 271
[35] Gabovich A M and Voitenko A I 1997 *Europhys. Lett.* **38** 371
[36] Wolf E L 1989 *Principles of Electron Tunnelling Spectroscopy* (Oxford: Oxford University Press)
[37] There are however some restrictions that it is important to take into account. They depend on the size of the ratio between the electron mean free path l and the radius of the constriction a. In the case where $l/2a \gg 1$, the regime is known as the ballistic regime. However, as was also studied by Kulik *et al* (see the reference below), in junctions where l is not much bigger than $2a$ (the thermal regime occurs when $l < 2a$) it is also possible to observe with a good resolution many of the electronic processes observed in the ballistic regime;
Kulik I O, Shekhter R I and Shkorbatov A G 1982 *Sov. Phys.–JETP* **54** 1130
[38] Bermon S and So C K 1978 *Solid State Commun.* **27** 723
[39] Tinkham M 1980 *Introduction to Superconductivity* (Malabar, FL: Krieger) p 45
[40] Meekes H 1988 *Phys. Rev.* B **38** 5924
[41] Moser M, Hullinger F and Wachter P 1985 *Physica* B **130** 21
[42] Moser M, Wachter P, Hullinger F and Etourneau J R 1985 *Solid State Commun.* **54** 241
[43] Moser M, Hullinger F and Wachter P 1985 *Physica* B **130** 21
[44] Frankowski I and Wachter P 1981 *Solid State Commun.* **40** 885
[45] Frankowski I and Wachter P 1982 *J. Appl. Phys.* **53** 7887
[46] Frankowski I and Wachter P 1982 *Solid State Commun.* **41** 577
[47] Bussian B, Frankowski I and Wohllenben D 1982 *Phys. Rev. Lett.* **49** 1026
[48] Morales F, Escudero R, Briggs A, Monceau P, Horyn R, Le Berre F and Peña O 1997 *Physica* B **218** 193
[49] Escudero R 1993 *Advanced Topics in Materials Science and Engineering* (New York: Plenum) p 195
[50] Appelbaum J 1966 *Phys. Rev. Lett.* **17** 91
[51] Anderson P W 1966 *Phys. Rev. Lett.* **17** 95
[52] McMillan W L 1981 *Phys. Rev.* B **24** 2739
McMillan W L and Mochel J 1981 *Phys. Rev. Lett.* **46** 556
[53] White A L, Dynes R C and Garno J P 1986 *Phys. Rev. Lett.* **56** 532
[54] Schmitz S and Ewert S 1991 *Solid State Commun.* **79** 525
[55] Hatta E, Tonokawa M, Nagao J and Mukasa K 1997 *Solid State Commun.* **102** 437
[56] Lee P A and Ramakrishnan T V 1985 *Rev. Mod. Phys.* **57** 287
[57] Raychaudhari A K 1995 *Adv. Phys.* **44** 21
[58] Altshuler B L and Aronov A G 1979 *Zh. Eksp. Teor. Fiz.* **77** 2028